water

MDPI

Article

Photoinhibition of the Picophytoplankter *Synechococcus* Is Exacerbated by Ocean Acidification

He Li [1], John Beardall [2] and Kunshan Gao [1,3,*]

[1] State Key Laboratory of Marine Environmental Science, College of Ocean and Earth Sciences, Xiamen University, Xiamen 361102, China
[2] School of Biological Sciences, Monash University, Clayton, VIC 3800, Australia
[3] Co-Innovation Center of Jiangsu Marine Bio-industry Technology, Jiangsu Ocean University, Lianyungang 222000, China
* Correspondence: ksgao@xmu.edu.cn

Abstract: The marine picocyanobacterium *Synechococcus* accounts for a major fraction of the primary production across the global oceans. However, knowledge of the responses of *Synechococcus* to changing pCO_2 and light levels has been scarcely documented. Hence, we grew *Synechococcus* sp. CB0101 at two CO_2 concentrations (ambient CO_2 AC:410 µatm; high CO_2 HC:1000 µatm) under various light levels between 25 and 800 µmol photons m^{-2} s^{-1} for 10–20 generations and found that the growth of *Synechococcus* strain CB0101 is strongly influenced by light intensity, peaking at 250 µmol m^{-2} s^{-1} and thereafter declined at higher light levels. *Synechococcus* cells showed a range of acclimation in their photophysiological characteristics, including changes in pigment content, optical absorption cross section, and light harvesting efficiency. Elevated pCO_2 inhibited the growth of cells at light intensities close to or greater than saturation, with inhibition being greater under high light. Elevated pCO_2 also reduced photosynthetic carbon fixation rates under high light but had smaller effects on the decrease in quantum yield and maximum relative electron transport rates observed under increasing light intensity. At the same time, the elevated pCO_2 significantly decreased particulate organic carbon (POC) and particulate organic nitrogen (PON), particularly under low light. Ocean acidification, by increasing the inhibitory effects of high light, may affect the growth and competitiveness of *Synechococcus* in surface waters in the future scenario.

Keywords: carbon fixation; elevated pCO_2; growth; light; photoinhibition; *Synechococcus*

check for updates

Citation: Li, H.; Beardall, J.; Gao, K. Photoinhibition of the Picophytoplankter *Synechococcus* Is Exacerbated by Ocean Acidification. *Water* **2023**, *15*, 1228. https://doi.org/10.3390/w15061228

Academic Editors: José Luis Sánchez-Lizaso and Rolf D. Vogt

Received: 23 February 2023
Revised: 17 March 2023
Accepted: 20 March 2023
Published: 21 March 2023

Copyright: © 2023 by the authors. Licensee MDPI, Basel, Switzerland. This article is an open access article distributed under the terms and conditions of the Creative Commons Attribution (CC BY) license (https://creativecommons.org/licenses/by/4.0/).

1. Introduction

The cyanobacteria *Synechococcus* and *Prochlorococcus* are the two most abundant marine pico-prokaryotic photosynthetic organisms and make up a significant portion of the marine phytoplankton community [1,2]. Compared to *Prochlorococcus*, *Synechococcus* has a wider geographical distribution that even covers both polar and high-nutrient waters [2–4], possibly related to its larger genome with more genomic plasticity that allows it to occupy more highly dynamic environments [3,5,6]. *Synechococcus* contributes approximately 17% of the primary production of the global ocean and fuels the food web and biological carbon pump, which plays a key role in the marine ecosystem [1,7].

The oceans have absorbed approximately 30% of the total anthropogenic emissions of CO_2 since the Industrial Revolution [8], driving a decrease in pH and changes in other carbonate chemistry parameters, a process termed Ocean Acidification (OA). Since the preindustrial era, the pH of surface ocean waters has dropped by 0.1 unit, and such a trend will see the global oceanic pH further reduced by 0.3–0.4 units by the end of 2100 under the "business-as-usual" scenario [9,10]. Coastal and estuarine waters are more susceptible to OA from anthropogenic activities than pelagic systems [11]. Elevated CO_2 from organic matter re-mineralized by microbial respiration processes further raises acidity,

with an additional drop in pH of 0.05 units, which reduces the buffering ability of coastal waters [11,12].

Most photoautotrophic phytoplankton possess CO_2 concentrating mechanisms (CCMs) to increase the CO_2 concentration at the Rubisco active site and overcome the supply limitation of CO_2 [13]. Although it is generally accepted that OA could alleviate the CO_2 limitation or/and downregulate the CCMs, which could save energy for other metabolic processes [14], laboratory studies show that ocean acidification has distinct effects on different species [15]. While photosynthesis buffers the effects of OA by forming a high pH micro-boundary and benefits from elevated CO_2 at the cell surface [16] in the daytime, enhanced respiration stimulated by OA releases CO_2, aggravating the acidic stress during the night period [17]. Thus, the observable effects of OA depend on the balance between the positive impacts of CO_2 enrichment and the negative impacts of lowered pH [18].

Moreover, the effects of OA could also be modulated by other environmental factors. It has been shown that elevated pCO_2 stimulates the quantum yield and growth rate of diatoms under low light, but under bright sunlight growth is inhibited and cells exhibit higher levels of nonphotochemical quenching [19]. In *Emiliania huxleyi*, elevated pCO_2 enhances growth, regardless of the different levels of incident solar visible radiation, and high light exposure could offset the negative effects of OA on calcification [20]. In macroalgae, most species tested so far exhibited enhanced or unchanged rates of growth and/or photosynthesis under the influences of OA and high light [21]. However, the effect of OA on *Synechococcus* has been poorly documented, though there have been some studies on the interactive effects of OA with other stressors on growth and physiology, including temperature [22,23], nutrients [24], and light [25,26]. In the context of future climate changes, the global model predicts that *Synechococcus* will occupy a wider niche distribution with a 14% increase in cell abundance by the end of the century [1]. Given its ecological importance and wide distribution, it is necessary to further study this picophytoplankton group in response to the interaction between OA and light.

The *Synechococcus* sp. CB0101 used in the present work was isolated from Chesapeake Bay, where the nutrients, temperature, and light intensity are highly variable [27,28]. Carbon dioxide and light are necessary for photosynthesis, so understanding how the picophytoplankton respond to these two environmental stressors is important for understanding the function of *Synechococcus* in marine ecosystems. Considering that rapid mixing of the water column can expose *Synechococcus* to dynamic changes in light during the daytime, we hypothesized that it could tolerate high light levels but might show a differential response to the combined effects of elevated pCO_2 (OA) and light intensity. Hence, in the present study, we manipulated various light levels and two pCO_2 levels to mimic the dynamic environment to investigate the physiological performance of a strain of *Synechococcus*.

2. Materials and Methods

2.1. Cultures and Experimental Design

The culture of *Synechococcus* strain CB0101 was originally isolated from Chesapeake Bay [29]. Cells were grown in glass flasks at 23 °C under a 12:12 light and dark cycle (7:00–19:00) in an incubator (GXZ280, Jiangnan Instrument Factory, Ningbo, China) and kept in an exponential growth phase by regular dilution using autoclaved seawater enriched with *Synechococcus* medium (SN15 medium) [30]. The cultures were illuminated by cool white LEDs (400–700 nm) and conducted at six light intensities (25, 50, 150, 250, 400, and 800 µmol photons m^{-2} s^{-1}), which were obtained by adjusting the distance from the light source and/or covering flasks with neutral density filters. The irradiance was measured with a Solar Light sensor (PAM2100, Solar light Co. Inc., Glenside, PA, USA).

Before inoculation, the culture medium was pre-equilibrated with 0.2–µm–filtered air with two pCO_2 levels of 410 (outdoor ambient air, AC) and 1000 µatm (predicted for the end of the century, HC) respectively, which were generated with a customized CO_2 enricher (CE100D, Ruihua Instrument & Equipment Co. Ltd., Wuhan, China). The elevated pCO_2

level is based on the higher end of predicted values in the Representative Concentration Pathway 8.5 (RCP8.5) emission scenario [10]. Cells were continuously bubbled with the target pCO_2 level during the experiment to ensure the stability of the seawater carbonate systems in cultures (Table S1). Triplicate cultures (400 mL) were exposed to each light and pCO_2 combination.

2.2. Carbonate Chemistry System

To determine the stability of the carbonate system in cultures, pH was measured by a pH meter (Orion 2 STAR; Thermo Fisher Scientific. Inc., Waltham, MA. USA), which was three-point calibrated with standard National Bureau of Standards (NBS) buffer. Total alkalinity (TA) was measured by Gran acidimetric titration with a TA analyzer (AS-Alk1+, Apollo SciTech, LLC, Newark, NJ, USA). Other parameters of the carbonate system were derived from pH_{NBS} and TA data with CO2SYS [31]. All the carbonate chemistry parameters are shown in Table S1.

2.3. Growth Rates

The cell concentration of cultures was monitored by a flow cytometer (CytoFLEX S, Beckman Coulter, Inc., Brea, CA, USA) following Bao and Gao [25]. The specific growth rate of each replicate was calculated from the logarithmic change in cell density, as described below.

$$\mu = (\ln N - \ln N_0)/(T - T_0), \quad (1)$$

in which N and N_0 are cell densities at times T and T_0, respectively.

The non-linear fitting of specific growth rates to growth light levels was performed using the following formula [32]:

$$\mu = \mu_{max} \times e^{-\alpha \times PAR/\mu max} \times e^{\beta \times PAR/\mu max}, \quad (2)$$

where PAR is the growth light intensity. The values of μ_{max}, α, and β are the model parameters obtained by fitting the growth data to the double exponential function above, and indicate maximal growth rate, light use efficiency, and growth photoinhibition coefficient, respectively.

2.4. Chlorophyll a Content and Optical Absorption Cross Section

Cells were collected on GF/F filters (Whatman, UK) under low vacuum pressure (<0.01 MPa) and then extracted in pure methanol overnight at 4 °C in darkness. The supernatant after centrifugation at 6000× *g* for 10 min at 4 °C was scanned for absorbance at 665 and 750 nm by using a spectrophotometer (TU1810, General Analytical Co. Ltd., Beijing, China). The concentrations of chlorophyll *a* (Chl *a*) were calculated according to Ritchie [33].

The optical absorption cross section (a^*) was determined by the quantitative filter technique [34]. The cell samples were filtered onto GF/F filters and scanned from 400 to 800 nm using a spectrophotometer equipped with an integrating sphere (Lambda950, PerkinElmer, Inc., Waltham, MA, USA). The same filters moistened with fresh culture medium were used as blanks. The absorption coefficient $a^*(\lambda)$ (m^2 $cell^{-1}$) normalized to cell [35] was calculated as

$$a^*(\lambda) = \frac{2.303 \cdot [OD(\lambda) - OD(750)] \cdot A}{\beta \cdot V \cdot (cell)}, \quad (3)$$

where the factor 2.303 converts from lg to ln and OD(λ) and OD(750) are the optical density of the samples at wavelengths λ and 750 nm, respectively. V (m^3) is the filtration volume of the sample, 'cell' is the cell concentration, A is the measured interception area of filter (m^2), and correction factor (β) accounts for the pathlength amplification parameter [35].

The mean absorption, $\bar{a}^*$, was obtained by averaging over the spectrum from 400 to 700 nm for comparison among different treatments as follows

$$a^* = \frac{1}{300}\sum_{400}^{700} a^*(\lambda)\ \Delta\lambda \quad (4)$$

Furthermore, absorption spectra $a^*(\lambda)$ can be described by a series of Gaussian curves to obtain the equations of Gauss peak spectra for quantifying the constituents of optical absorption cross section [34,36], and thus calculate the relative contribution of different pigments to $a^*(\lambda)$ (Figure S2).

2.5. Chlorophyll a Fluorescence

The photochemical parameters were measured in the middle of the photoperiod within 2 h with a Multi-Color Pulse-Amplitude-Modulated chlorophyll fluorometer using blue (440 nm) to excite Chl *a* (Multi-color-PAM, Heinz Walz GmbH, Effeltrich, Germany). The saturation pulse was set at 5000 µmol photons m^{-2} s^{-1} and lasted for 800 ms. Effective photochemical quantum yield (Φ_{PSII}), indicating photosystem II activity, was determined by measuring the steady-state chlorophyll fluorescence (F_t) and the instant maximum fluorescence (F_m') under the growth-light-adapted state. The quantum yield was calculated according to the equation [37]:

$$F_v'/F_m' = (F_m' - F_t)/F_m' \quad (5)$$

The relative electron transport rate (rETR) of the cells under different treatments was assessed as: $rETR = \Phi_{PSII} \times PFD$, where Φ_{PSII} is the effective quantum yield at each actinic light intensity (PFD), ranging from 0 to 2855 µmol photons m^{-2} s^{-1} with a duration of 20 s at each step. The rapid light curve of rETR was fitted according to the model of Eilers and Peeters [38]:

$$rETR = PAR/(a \times PAR^2 + b \times PAR + c), \quad (6)$$

where *a*, *b*, *c* are the model parameters. The photosynthetic light-harvesting efficiency (α), maximum electron transport rate ($rETR_{max}$), and light saturation point (I_k) were calculated from *a*, *b*, and *c*. (Figure S1)

2.6. Carbon Fixation Rates

Carbon fixation rates of cells were measured using the ^{14}C method [22]. Approximately 20 mL of samples were dispensed into 25 mL borosilicate bottles and inoculated with 5 µCi (0.185 MBq) of labeled sodium bicarbonate (PerkinElmer, Inc., Waltham, MA, USA). After 2 h of incubation in the middle of the photoperiod under the respective experimental growth conditions, samples were immediately filtered onto Whatman GF/F filters under dim light. The filters were then placed in 20 mL scintillation vials, exposed to HCl fumes overnight, and dried at 60 °C for 5 h. Scintillation fluid (Hisafe 3, PerkinElmer, Inc., Waltham, MA, USA) was added to the vials before measuring the incorporated radioactivity with a liquid scintillation counter (Tri-Carb 2800TR, PerkinElmer, Inc., Waltham, MA, USA).

2.7. C and N Analysis

After the exponentially grown cells had been acclimated to the growth conditions for approximately 10 generations, samples for particulate organic carbon (POC) and particulate organic nitrogen (PON) were harvested onto pre-combusted (450 °C for 6 h) GF/F filters and stored at −80 °C until analysis. Filters were exposed to HCl fumes overnight to remove inorganic carbon and then dried at 60 °C for 12 h. The filters were packed into tin cups and analyzed with a CHNS/O elemental analyzer (Vario EL cube, Elementar Analysensysteme GmbH, Frankfurt, Germany).

2.8. Data Analysis

Two-way ANOVA was used with SPSS software (version 18.0) to determine the individual effects of pCO_2 and light levels and their interactions. When $p < 0.05$, a Tukey test was conducted as a post hoc (One-way ANOVA) test to analyze significant differences among the treatments. All data were presented as the means ± SD of three independent cultures.

3. Results

3.1. Growth and Chl *a*

Two-way ANOVA analysis indicated there were significant individual and interactive effects of pCO_2 and light on the specific growth rate of *Synechococcus* sp. CB0101 (Table S3, Two-way ANOVA, $p < 0.001$, $p < 0.001$, $p < 0.001$, respectively). After the 10 generations of acclimation at the two pCO_2 levels and various light intensities, the growth rate of *Synechococcus* was lowest at 25 μmol photons m^{-2} s^{-1} (Figure 1). The growth of cells in both AC and HC treatments increased with the increased levels of light, peaking at 250 μmol m^{-2} s^{-1} (2.17 d^{-1} for AC, 2.06 d^{-1} for HC), and thereafter declined at light intensities above this optimal point. Compared to the highest growth rate at 250 μmol m^{-2} s^{-1}, the growth rate at 800 μmol m^{-2} s^{-1} was decreased by 24% and 29% under AC and HC conditions, respectively (Tukey test, $p < 0.001$, $p < 0.001$). Growth rates were unaffected by HC up to 150 μmol photons m^{-2} s^{-1}, but above this, HC resulted in a significant drop in growth rate, with a 5%, 8%, and 11% decline at 250, 400, and 800 μmol m^{-2} s^{-1}, respectively (Tukey test, $p = 0.001$, $p < 0.001$, $p < 0.001$).

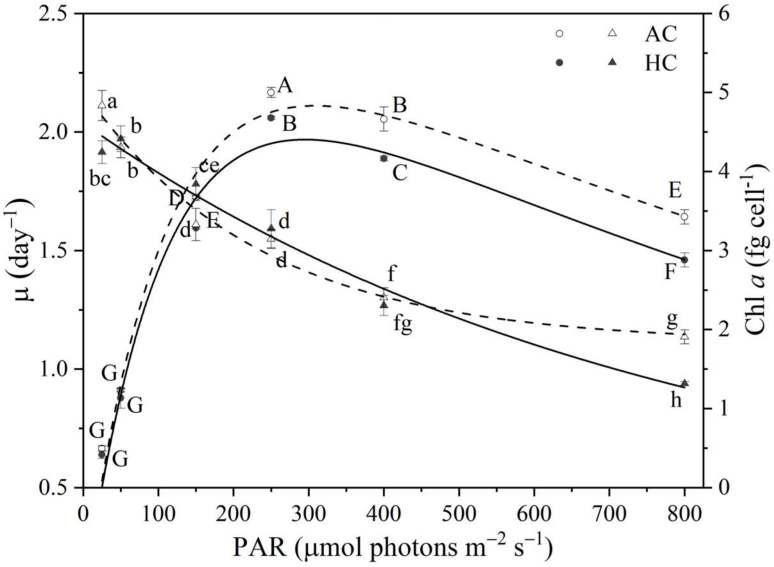

Figure 1. Specific growth rate (μ) (circles) and chlorophyll *a* content (triangles) of *Synechococcus* CB0101 grown under different light levels combined with the ambient (AC, 415 μatm, the dotted line) or elevated pCO_2 (HC, 1000 μatm, the solid line). The values are means ± SD of triplicate cultures. Different letters (uppercase for μ, lowercase for Chl *a*) indicate significant ($p < 0.05$) differences among the treatments.

The Chl *a* content of *Synechococcus* decreased with increasing light levels under both AC and HC conditions (Figure 1, Table S3, Two-way ANOVA, $p < 0.001$). Compared with the AC treatment, elevated pCO_2 only significantly enhanced Chl *a* content under 150 μmol photons m^{-2} s^{-1} ($p = 0.022$) but decreased the Chl *a* content by 12% ($p = 0.005$) and 31% ($p < 0.001$) under 25 and 800 μmol m^{-2} s^{-1} levels, respectively. In both AC and HC treatments, the Chl *a* contents at 800 μmol m^{-2} s^{-1} were 61% and 69% lower than that under the lowest light intensity, respectively (Tukey test, $p < 0.001$, $p < 0.001$).

3.2. Carbon Fixation

Similar to the growth rate, the photosynthetic carbon fixation rate per cell, measured at the growth light intensity, typically increased with light from 0.68 and 0.81 to a maximum of 4.46 and 2.85 fmol C cell^{-1} h^{-1} under AC and HC treatments, respectively, and then declined rapidly under the highest light intensity applied (Figure 2a). Under both AC and HC conditions, the carbon fixation rate at 800 µmol m^{-2} s^{-1} was significantly decreased by 50% and 51% compared with that of cells at 250 µmol m^{-2} s^{-1}, respectively (Tukey test, $p < 0.001$, $p < 0.001$). Elevated pCO_2 did not change the carbon fixation significantly up to 150 µmol photons m^{-2} s^{-1} but showed a significant decline in fixation rate by 39%, 46%, and 38% under 250, 400, and 800 µmol m^{-2} s^{-1}, respectively (Figure 2a, Tukey test, $p < 0.001$, $p < 0.001$, $p < 0.001$). The photoinhibition coefficient (β) under AC (0.0044) was higher than that at elevated pCO_2 (0.0025) (Table 1). The same trend with light was observed when the carbon fixation was normalized to Chl *a* content (Figure 2b).

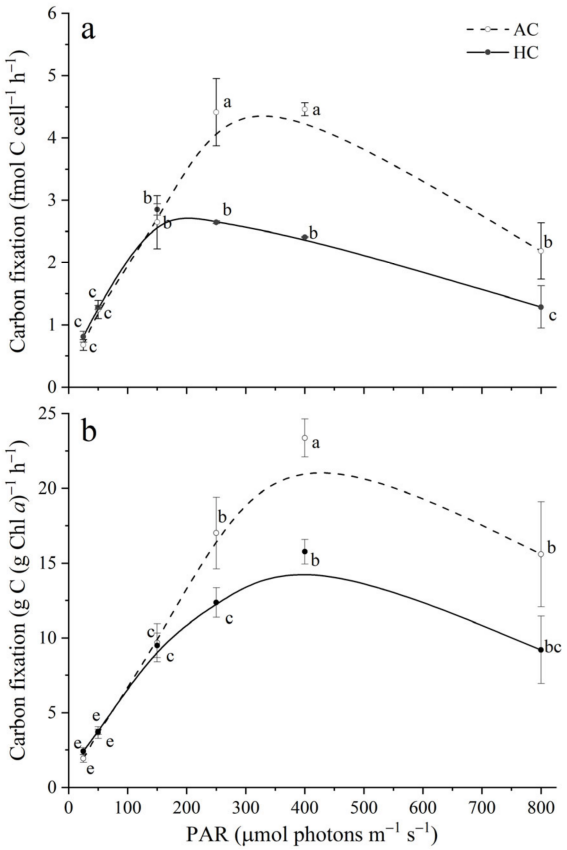

Figure 2. Photosynthetic carbon fixation of *Synechococcus* per cell (**a**) or per Chl *a* (**b**) grown under different light levels combined with the ambient (AC, 415 µatm, the dotted line) or elevated (HC, 1000 µatm, the solid line) pCO_2. The values are means ± SD of triplicate cultures. Different letters indicate significant ($p < 0.05$) differences among the treatments.

Table 1. The light harvesting efficiency (α) and photoinhibitory coefficient (β) of *Synechococcus* CB0101 grown under different light levels combined with ambient (AC, 415 µatm) or elevated pCO_2 (HC, 1000 µatm), derived from the growth and carbon fixation curves at the growth intensity (Figures 1 and 2a), respectively.

	Growth		Carbon Fixation	
	AC	**HC**	**AC**	**HC**
α	0.0246 ± 0.0006	0.0234 ± 0.0017	0.0146 ± 0.0028	0.0295 ± 0.0013
β	0.0010 ± 0.0001	0.0011 ± 0.0001	0.0044 ± 0.0010	0.0025 ± 0.0006

3.3. Chlorophyll a Fluorescence

Although the interaction of pCO_2 and light suggested a significant effect on effective quantum yield and α (Figure 3a,b, Table S3, Two-way ANOVA, $p < 0.001$, $p = 0.022$), there was no significant interaction of pCO_2 and light on $rETR_{max}$ (Figure 3c, $p = 0.063$). The increase in light intensity significantly reduced effective quantum yield and α (Table S3, Two-way ANOVA, $p < 0.001$), while elevated pCO_2 enhanced the values at all the light levels (Two-way ANOVA, $p < 0.001$). $rETR_{max}$ showed a similar pattern among different treatments as was found for growth, which increased with light and reached a plateau. In general, elevated pCO_2 had significant positive effects on effective quantum yield, α, and $rETR_{max}$, suggesting that elevated pCO_2 improved light absorption capacity. There were close correlations between carbon fixation or growth rate and $rETR_{max}$ (Figure 4).

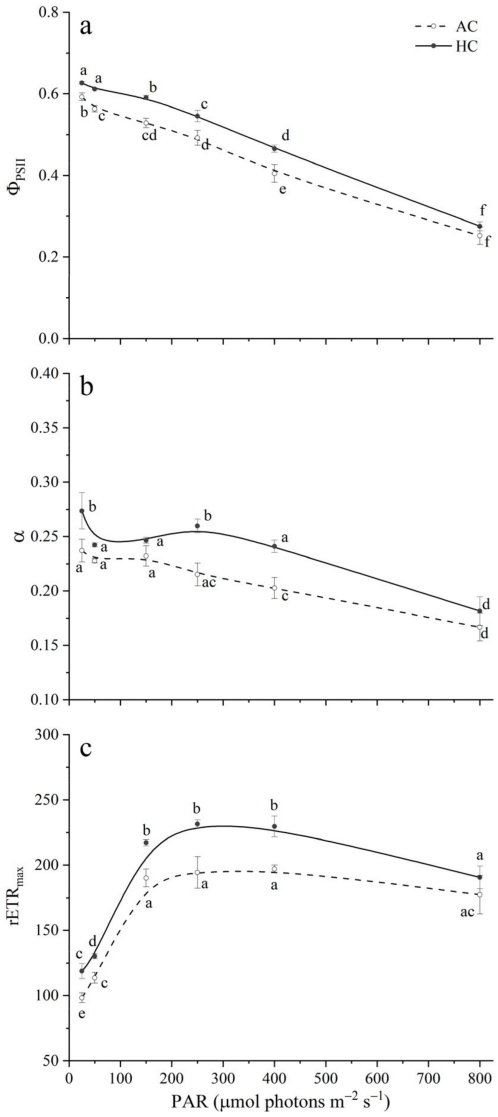

Figure 3. The effective quantum yield (Φ_{PSII}) (**a**) and photosynthetic light-harvesting efficiency (α) (**b**), maximum electron transport rate ($rETR_{max}$) (**c**) of *Synechococcus* cells grown under different light levels combined with the ambient (AC, 415 μatm, the dotted line) or elevated pCO_2 (HC, 1000 μatm, the solid line). The α and $rETR_{max}$ parameters were derived from rapid light curves (see Figure S1 and Table S2). The values are means ± SD of triplicate cultures. Different letters indicate significant ($p < 0.05$) differences among the treatments.

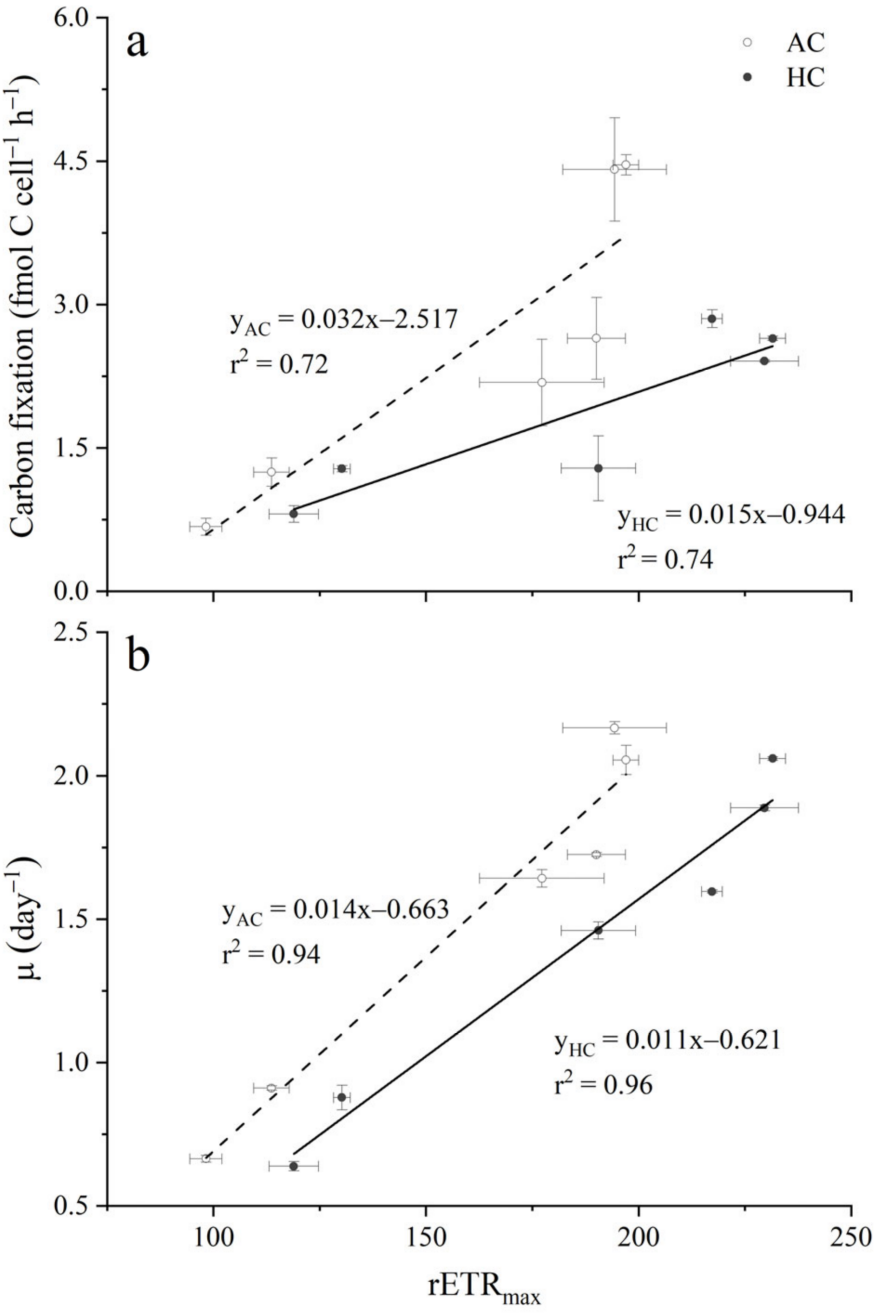

Figure 4. Plots of carbon fixation rate (**a**) and growth rate (**b**) versus $rETR_{max}$ of *Synechococcus* CB0101 grown under different light levels combined with the ambient (AC, 415 μatm, the dotted line) or elevated (HC, 1000 μatm, the solid line) pCO_2. The values are means ± SD of triplicate cultures. There were close correlations between carbon fixation or growth rate and $rETR_{max}$.

3.4. Optical Absorption Cross Section

Two-way ANOVA showed that pCO_2 and light had significant individual and interactive effects on mean absorption, $\bar{a}^*$, per cell between 400 and 700 nm (Table S3, Two-way ANOVA, $p < 0.001$, $p < 0.001$, $p < 0.001$). The $\bar{a}^*$ values ranged from 0.470 to 1.877 × 10^{-13} m^2 $cell^{-1}$ among these different treatments (Figure 5a). Under both AC and HC conditions, $\bar{a}^*$ showed a decreased trend with increasing light intensity. The contributions of each major pigment to a^* obtained by Gaussian function analysis were different among culture conditions (Figure 5b,c). The contributions of Chl *a* ranged from 53% to 77%, while the contributions of PC decreased from 29% to 11% with increasing light under AC and HC

conditions, respectively. In general, high light levels enhanced the relative contribution of Chl *a* but reduced the phycobilin contributions, which showed an increasing trend in Chl *a*/(PE + PC) ratio (Figure 5d). However, elevated pCO_2 increased the relative contributions of total phycobilins under high light levels.

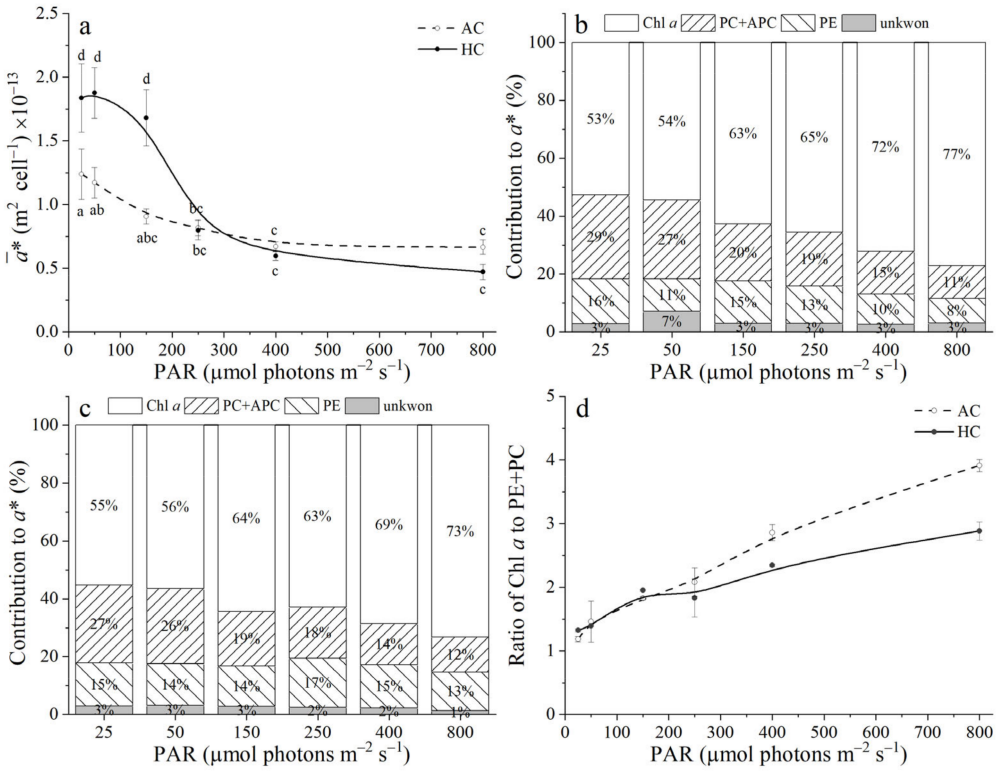

Figure 5. The average optical absorption cross section ($\bar{a}^*$) per cell (**a**), relative contributions ((**b**) for AC, (**c**) for HC) to $\bar{a}^*$ by different pigments, and the ratio of Chl *a* to phycobilins (**d**) in *Synechococcus* cells grown under different light levels combined with the ambient (AC, 415 μatm, the dotted line) or elevated (HC, 1000 μatm, the solid line) pCO_2. The values are means ± SD of triplicate cultures. Different letters indicate significant ($p < 0.05$) differences among the treatments.

3.5. Cellular POC Content and POC

In both AC and HC treatments, POC decreased with increasing light levels, respectively (Figure 6a, Table S3, Two-way ANOVA, $p < 0.001$). The cellular POC content decreased by 40% and 27% at 800 μmol m^{-2} s^{-1} compared with 25 μmol m^{-2} s^{-1} under AC and HC condition, respectively (Tukey test, $p < 0.001$, $p = 0.004$). Elevated pCO_2 decreased the cellular POC significantly only at 50 and 150 μmol m^{-2} s^{-1} (Tukey test, $p = 0.002$, $p = 0.037$). Similar to the cellular POC content, the cellular PON decreased with increasing light intensity in both HC- and AC-grown cells of *Synechococcus* (Figure 6b). The C:N ratio showed an increasing trend, ranging from 4.16 to 5.56, with light intensity. Elevated pCO_2 only decreased the C:N ratio significantly by 14% at 800 μmol m^{-2} s^{-1} ($p < 0.001$). In addition, a significant interaction between pCO_2 and light levels on the C:N ratio was observed (Figure 6c, Table S3, Two-way ANOVA, $p = 0.002$).

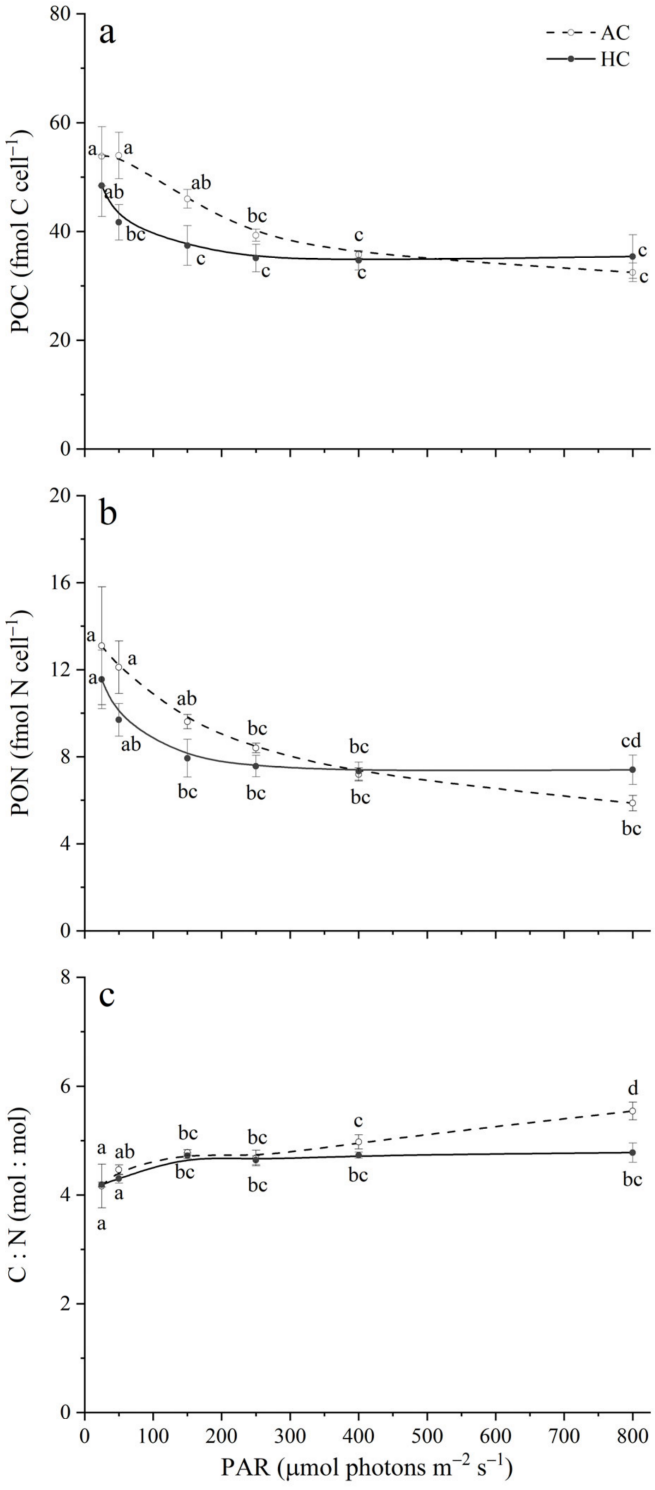

Figure 6. Particulate organic carbon (POC) (**a**) and nitrogen (PON) (**b**) and the C:N ratio (mol:mol) (**c**) of *Synechococcus* cells grown under different light levels combined with the ambient (AC, 415 μatm, the dotted line) or elevated (HC, 1000 μatm, the solid line) pCO_2. The values are means ± SD of triplicate cultures. Different letters indicate significant ($p < 0.05$) differences among the treatments.

4. Discussion

Our findings demonstrated that the growth and carbon fixation of *Synechococcus* sp. CB0101 increased with light intensity up to an optimum, beyond which values decreased

with increasing growth light. *Synechococcus* could decrease pigments and optical absorption cross section (mean absorption $\bar{a}^*$ per cell) to diminish energy uptake to protect the photosystems. Although elevated pCO_2 improved the electron transfer rates (rETR), it exacerbated the depression of the carbon fixation and ultimately decreased the growth of *Synechococcus* cells under the high light intensities used, indicating a decrease in energy transfer efficiency under ocean acidification.

Synechococcus strain CB0101 has strong plasticity to light in its aquatic habitats with sharp fluctuations in light intensity exposure, retaining a high growth rate under high light intensity (Figure 1). It acclimates by changes in the contents of cellular constituents, such as proteins and pigments, or by state transitions, to cope with its variable growth light environment [39,40]. In this work, the Chl *a* content and $\bar{a}^*$ per cell of *Synechococcus* decreased rapidly with the increased light intensity under both ambient and elevated pCO_2 levels (Figures 1 and 5a). Cyanobacteria also change their light absorption coefficients and modify the composition of pigments during photo-acclimation (Figure 5b,c). Thus, under AC and HC conditions, the contribution of Chl *a* to a^* increased gradually, whereas the phycobilin contributions declined with the increased light levels, resulting in an increasing ratio of Chl *a*/(PE + PC) (Figure 5d). The decrease in phycobilins reflects the reduction in phycobilisome antenna size. These changes effectively diminish energy uptake and play a protective role in the photosynthetic system, alleviating the potential for photoinhibition caused by high light [41].

Light is the primary energy source for cell metabolism in photosynthetic organisms. Photosynthesis uses light energy to generate ATP and NADPH, which are partly consumed with the conversion of CO_2 as sugar to support metabolic activities [42]. Changes in the photosystem stoichiometry of cyanobacteria by adjusting the PS I/PS II ratio, or in the balance of electron flow between PS II and PS I, contribute to the optimization of photosynthetic efficiency to adapt well to different light regimes [42,43]. The effective quantum yield and light-use efficiency (α) of *Synechococcus* adapted to the prevailing light-growth conditions decreased with increasing growth light levels (Figure 3a,b), which could regulate and maintain the relative electron transport rates across optimal and supersaturated growth light levels (Figure 3c). On the other hand, photophysiological parameters such as effective quantum yield, α, and $rETR_{max}$ were enhanced under elevated pCO_2 (Figure 3). The fact that there was additional electron drainage (leading to a higher rETR) in HC-grown cells [25,44], which means a more rapid energy supply, suggests enhancement of CO_2 assimilation and/or photorespiration. The results were further confirmed by the high carbon fixation rates with increased light levels, which have previously been shown in *Synechococcus* [26]. The electron transport rates showed a close correlation with carbon fixation and specific growth rates (Figure 4). Although HC treatment increased the electron transport rates, α values from growth vs. light curve, the slope of the correlation between electron transport rates and growth rates were lower under acidification than those in AC grown cells, suggesting that HC ultimately exacerbates the decrease in energy transfer efficiency (Table 1 and Figure 4).

Cyanobacteria such as *Synechococcus* also possess active CO_2 concentrating mechanisms (CCMs) [45]. The energy saved by the downregulation of CCMs due to increased external CO_2 availability is expected to promote carbon fixation and growth, especially with the limitation of energy generation under low light [19]. In this work, elevated pCO_2 enhanced the carbon fixation rate of cells by 4–21% under low light (Figure 2a, Table S4), which is consistent with previous reports [22,46]. Although the allocation of energetic savings by CCMs downregulating is beneficial for *Synechococcus*, the lowered pH consequent on elevated pCO_2 imposes additional energetic costs in cells to maintain cytosolic pH homeostasis and external acidic stress, which was aggravated during the night due to the higher respiratory CO_2 release under HC condition [17,47–49]. Wu et al. [47] found that ocean acidification increased respiration by 30% to cope with the acidic stress in the diatom, resulting in respiratory carbon loss, which was consistent with 11–23% declines in

the stoichiometry of cellular POC of *Synechococcus* at elevated pCO_2 in our study, and thus reduced the growth rate compared to the AC treatment (Figures 1 and 6).

The energy supply from electron transport (rETR) increased with increasing light intensity, up to a plateau, but the carbon fixation rate peaked and then declined, indicating that high light caused photoinhibition (Figures 2 and 3c and Table 1). Meanwhile, elevated pCO_2 along with light stress diminishes energy dissipation via carbon acquisition due to downregulated CCMs, which would bring about additional photodamage and lower energy transfer efficiency (Figure 4) [19]. Because intracellular Ci pools are decreased in HC-grown algae [50,51], photorespiration could be enhanced because of the high O_2:CO_2 ratio around the Rubisco active site [44,52], thereby competing with carboxylation. Although we did not measure photorespiration in this work, the depressed carbon fixation of HC-grown cells (Figure 2) under excessive light levels could be partially due to increased photorespiratory rate, reflecting a strategy by which *Synechococcus* increased its defense against elevated pCO_2 by promoting energy dissipation under high light for sustaining the balance between carboxylation and oxygenation [44]. Due to the enhanced respiration, including dark and photo-respiration, caused by stressful light intensities [19], cellular POC and PON of *Synechococcus* eventually decreased with increasing moderate light intensities but levelled off at high light, even though the carbon fixation is relatively high under high light (Figures 2 and 6). Under HC conditions, cellular POC and PON were not decreased significantly under high light (greater than 400 μmol m^{-2} s^{-1}), despite the decline in growth rate (Figures 1 and 6). However, POC and PON production rates declined under all light levels at elevated pCO_2, which reduced the capacity for carbon and nitrogen export to the biogeochemical cycle in the ocean (Figure S3).

In general, our results indicate that *Synechococcus* CB0101 has a strong capacity for acclimation to light. The long-term cumulative effects should not be ignored given the high proportional contribution of *Synechococcus* to primary production [25]. Though increased pCO_2 decreases the growth rate only slightly, it would greatly reduce the primary productivity of *Synechococcus* that supports carbon export in the ocean under high light intensities. While coastal and estuarine habits where *Synechococcus* CB0101 is found are predicted to be acidified faster due to anthropogenic eutrophication [11], rapid mixing of the water column can expose the cells to cycles of high and low light conditions during the daytime, modulating the negative impact of OA on its carbon production and biomass, and thus reduce the competitiveness of this *Synechococcus* strain to cope with the complex water environment. Although the present work showed the tolerance of *Synechococcus* to light and acidic stress, multifactorial experiments, including concomitant environmental variations of nutrients and/or temperature, are required to further clarify the complex effects on *Synechococcus* strains in a changing future ocean.

5. Conclusions

In this work, when the picophytoplankter *Synechococcus* sp. CB0101 was acclimated to an elevated pCO_2 of 1000 μatm under different light levels, photosynthesis and growth were more inhibited at high light than under current ambient CO_2. The future acidification induced by elevated pCO_2 also significantly reduced cellular POC and PON, implying potential influences on biogeochemical cycles of C and N. While enhanced dark respiration and photorespiration could be responsible for the results, future work will investigate changes in the metabolic pathways responsible for the combined impacts of OA and high light on *Synechococcus* spp.

Supplementary Materials: The following supporting information can be downloaded at: https://www.mdpi.com/article/10.3390/w15061228/s1, Table S1: Carbonate chemistry parameters in the cultures of *Synechococcus* CB0101 grown under different light levels combined with the ambient or elevated pCO_2. Table S2: The photochemical parameters derived from rapid light curves (Figure S2) of *Synechococcus* cells grown under different pCO_2 and light combinations. Table S3: Statistical analyses of physiological traits of *Synechococcus* CB0101 grown under different pCO_2 and light combinations. Table S4: Percentage inhibition of carbon fixation under elevated pCO_2 under different light levels. Figure S1: Rapid light curve (RLC) of *Synechococcus* CB0101 grown under different light levels combined with the ambient or elevated pCO_2. Figure S2: An example of decomposition of the absorption spectra a*(λ) by a series of Gaussian curves. Figure S3: Particulate organic carbon (POC) and nitrogen (PON) production rates of *Synechococcus* CB0101 grown under different pCO_2 and light combinations. Figure S4: PCA analysis of rETR vs Irradiance data from Figure S1 for all treatments.

Author Contributions: Conceptualization, H.L. and K.G.; investigation, H.L.; data curation, H.L.; formal analysis, H.L. and J.B.; visualization, H.L.; writing—original draft preparation, H.L. and K.G.; writing—review and editing, H.L., K.G., and J.B.; project administration, K.G.; funding acquisition, K.G.; All authors have read and agreed to the published version of the manuscript.

Funding: This study was supported by the National Natural Science Foundation (41890803, 41721005, 41720104005).

Data Availability Statement: The data are available upon request to the corresponding author (Kunshan Gao).

Acknowledgments: We are grateful to Rui Zhang for providing the strain, and to the laboratory engineers Xianglan Zeng, Wenyan Zhao, and Liting Peng for their logistical and technical support.

Conflicts of Interest: The authors declare no conflict of interest.

References

1. Flombaum, P.; Gallegos, J.L.; Gordillo, R.A.; Rincón, J.; Zabala, L.L.; Jiao, N.; Karl, D.M.; Li, W.K.; Lomas, M.W.; Veneziano, D. Present and future global distributions of the marine Cyanobacteria *Prochlorococcus* and *Synechococcus*. *Proc. Natl. Acad. Sci. USA* **2013**, *110*, 9824–9829. [CrossRef] [PubMed]
2. Kim, Y.; Jeon, J.; Kwak, M.S.; Kim, G.H.; Koh, I.; Rho, M. Photosynthetic functions of *Synechococcus* in the ocean microbiomes of diverse salinity and seasons. *PLoS ONE* **2018**, *13*, e0190266. [CrossRef] [PubMed]
3. Partensky, F.; Blanchot, J.; Vaulot, D. Differential distribution and ecology of *Prochlorococcus* and *Synechococcus* in oceanic waters: A review. *Bull.-Inst. Oceanogr. Monaco-Numero Spec.* **1999**, *19*, 457–476.
4. Parli, B.V.; Bhaskar, J.T.; Jawak, S.; Jyothibabu, R.; Mishra, N. Mixotrophic plankton and *Synechococcus* distribution in waters around Svalbard, Norway during June 2019. *Polar Sci.* **2021**, *30*, 100697. [CrossRef]
5. Fucich, D.; Chen, F. Presence of toxin-antitoxin systems in picocyanobacteria and their ecological implications. *ISME J.* **2020**, *14*, 2843–2850. [CrossRef]
6. Wang, T.; Li, J.; Jing, H.; Qin, S. Picocyanobacterial *Synechococcus* in marine ecosystem: Insights from genetic diversity, global distribution, and potential function. *Mar. Environ. Res.* **2022**, *177*, 105622. [CrossRef]
7. Guidi, L.; Chaffron, S.; Bittner, L.; Eveillard, D.; Larhlimi, A.; Roux, S.; Darzi, Y.; Audic, S.; Berline, L.; Brum, J.R.; et al. Plankton networks driving carbon export in the oligotrophic ocean. *Nature* **2016**, *532*, 465–470. [CrossRef]
8. Howes, E.L.; Joos, F.; Eakin, C.M.; Gattuso, J.-P. An updated synthesis of the observed and projected impacts of climate change on the chemical, physical and biological processes in the oceans. *Front. Mar. Sci.* **2015**, *2*, 36. [CrossRef]
9. Orr, J.C.; Fabry, V.J.; Aumont, O.; Bopp, L.; Doney, S.C.; Feely, R.A.; Gnanadesikan, A.; Gruber, N.; Ishida, A.; Joos, F. Anthropogenic ocean acidification over the twenty-first century and its impact on calcifying organisms. *Nature* **2005**, *437*, 681–686. [CrossRef]
10. Gattuso, J.-P.; Magnan, A.; Billé, R.; Cheung, W.W.; Howes, E.L.; Joos, F.; Allemand, D.; Bopp, L.; Cooley, S.R.; Eakin, C.M. Contrasting futures for ocean and society from different anthropogenic CO_2 emissions scenarios. *Science* **2015**, *349*, aac4722. [CrossRef]
11. Cai, W.-J.; Hu, X.; Huang, W.-J.; Murrell, M.C.; Lehrter, J.C.; Lohrenz, S.E.; Chou, W.-C.; Zhai, W.; Hollibaugh, J.T.; Wang, Y. Acidification of subsurface coastal waters enhanced by eutrophication. *Nat. Geosci.* **2011**, *4*, 766–770. [CrossRef]
12. Feely, R.A.; Alin, S.R.; Newton, J.; Sabine, C.L.; Warner, M.; Devol, A.; Krembs, C.; Maloy, C. The combined effects of ocean acidification, mixing, and respiration on pH and carbonate saturation in an urbanized estuary. *Estuar. Coast. Shelf Sci.* **2010**, *88*, 442–449. [CrossRef]
13. Giordano, M.; Beardall, J.; Raven, J.A. CO_2 concentrating mechanisms in algae: Mechanisms, environmental modulation, and evolution. *Annu. Rev. Plant Biol.* **2005**, *56*, 99–131. [CrossRef]

14. Beardall, J.; Giordano, M. Ecological implications of microalgal and cyanobacterial CO_2 concentrating mechanisms, and their regulation. *Funct. Plant Biol.* **2002**, *29*, 335–347. [CrossRef]
15. Gao, K.; Gao, G.; Wang, Y.; Dupont, S. Impacts of ocean acidification under multiple stressors on typical organisms and ecological processes. *Mar. Life Sci. Technol.* **2020**, *2*, 279–291. [CrossRef]
16. McNicholl, C.; Koch, M.; Swarzenski, P.; Oberhaensli, F.; Taylor, A.; Batista, M.G.; Metian, M. Ocean acidification effects on calcification and dissolution in tropical reef macroalgae. *Coral Reefs* **2020**, *39*, 1635–1647. [CrossRef]
17. Raven, J.A.; Beardall, J.; Quigg, A. Light-Driven Oxygen Consumption in the Water-Water Cycles and Photorespiration, and Light Stimulated Mitochondrial Respiration. In *Photosynthesis in Algae: Biochemical and Physiological Mechanisms*; Larkum, A.W.D., Grossman, A.R., Raven, J.A., Eds.; Springer International Publishing: Cham, Switzerland, 2020; pp. 161–178.
18. Qu, L.; Beardall, J.; Jiang, X.; Gao, K. Elevated pCO_2 enhances under light but reduces in darkness the growth rate of a diatom, with implications for the fate of phytoplankton below the photic zone. *Limnol. Oceanogr.* **2021**, *66*, 3630–3642. [CrossRef]
19. Gao, K.; Xu, J.; Gao, G.; Li, Y.; Hutchins, D.A.; Huang, B.; Wang, L.; Zheng, Y.; Jin, P.; Cai, X.; et al. Rising CO_2 and increased light exposure synergistically reduce marine primary productivity. *Nat. Clim. Chang.* **2012**, *2*, 519–523. [CrossRef]
20. Jin, P.; Ding, J.; Xing, T.; Riebesell, U.; Gao, K. High levels of solar radiation offset impacts of ocean acidification on calcifying and non-calcifying strains of *Emiliania huxleyi*. *Mar. Ecol. Prog. Ser.* **2017**, *568*, 47–58. [CrossRef]
21. Ji, Y.; Gao, K. Effects of climate change factors on marine macroalgae: A review. *Adv. Mar. Biol.* **2021**, *88*, 91–136. [CrossRef]
22. Fu, F.X.; Warner, M.E.; Zhang, Y.; Feng, Y.; Hutchins, D.A. Effects of Increased temperature and CO_2 on photosynthesis, growth, and elemental ratios in marine *Synechococcus* and *Prochlorococcus* (cyanobacteria). *J. Phycol.* **2007**, *43*, 485–496. [CrossRef]
23. Basu, S.; Mackey, K.R. Effect of Rising Temperature and Carbon Dioxide on the Growth, Photophysiology, and Elemental Ratios of Marine *Synechococcus*: A Multistressor Approach. *Sustainability* **2022**, *14*, 9508. [CrossRef]
24. Mou, S.; Zhang, Y.; Li, G.; Li, H.; Liang, Y.; Tang, L.; Tao, J.; Xu, J.; Li, J.; Zhang, C. Effects of elevated CO_2 and nitrogen supply on the growth and photosynthetic physiology of a marine cyanobacterium, *Synechococcus* sp. PCC7002. *J. Appl. Phycol.* **2017**, *29*, 1755–1763. [CrossRef]
25. Bao, N.; Gao, K. Interactive effects of elevated CO_2 concentration and light on the picophytoplankton *Synechococcus*. *Front. Mar. Sci.* **2021**, *8*, 634189. [CrossRef]
26. Laws, E.A.; McClellan, S.A. Interactive effects of CO_2, temperature, irradiance, and nutrient limitation on the growth and physiology of the marine cyanobacterium *Synechococcus* (Cyanophyceae). *J. Phycol.* **2022**, *58*, 703–718. [CrossRef]
27. Wang, K.; Wommack, K.E.; Chen, F. Abundance and distribution of *Synechococcus* spp. and cyanophages in the Chesapeake Bay. *Appl. Environ. Microb.* **2011**, *77*, 7459–7468. [CrossRef]
28. Marsan, D.; Wommack, K.E.; Ravel, J.; Chen, F. Draft genome sequence of *Synechococcus* sp. strain CB0101, isolated from the Chesapeake Bay estuary. *Genome Announc.* **2014**, *2*, e01111-13. [CrossRef]
29. Chen, F.; Wang, K.; Kan, J.; Bachoon, D.S.; Lu, J.; Lau, S.; Campbell, L. Phylogenetic diversity of *Synechococcus* in the Chesapeake Bay revealed by Ribulose-1, 5-bisphosphate carboxylase-oxygenase (RuBisCO) large subunit gene (rbcL) sequences. *Aquat. Microb. Ecol.* **2004**, *36*, 153–164. [CrossRef]
30. Waterbury, J.B. Biological and ecological characterization of the marine unicellular cyanobacterium *Synechococcus*. *Can Bull. Fish Aquat. Sci.* **1986**, *214*, 71–120.
31. Lewis, E.; Wallace, D. Program Developed for CO_2 System Calculations; Environmental System Science Data Infrastructure for a Virtual Ecosystem. 1998. Available online: https://www.osti.gov/servlets/purl/639712 (accessed on 8 March 2023).
32. Platt, T.; Gallegos, C.; Harrison, W.G. Photoinhibition of photosynthesis in natural assemblages of marine phytoplankton. *J. Mar. Res.* **1980**, *38*, 687–701.
33. Ritchie, R.J. Consistent sets of spectrophotometric chlorophyll equations for acetone, methanol and ethanol solvents. *Photosynth. Res.* **2006**, *89*, 27–41. [CrossRef]
34. Subramaniam1, A.; Carpenter, E.J.; Karentz, D.; Falkowski, P.G. Bio-optical properties of the marine diazotrophic cyanobacteria *Trichodesmium* spp. I. Absorption and photosynthetic action spectra. *Limnol. Oceanogr.* **1999**, *44*, 608–617. [CrossRef]
35. Stramski, D.; Reynolds, R.A.; Kaczmarek, S.; Uitz, J.; Zheng, G. Correction of pathlength amplification in the filter-pad technique for measurements of particulate absorption coefficient in the visible spectral region. *Appl. Opt.* **2015**, *54*, 6763–6782. [CrossRef]
36. Küpper, H.; Seibert, S.; Parameswaran, A. Fast, sensitive, and inexpensive alternative to analytical pigment HPLC: Quantification of chlorophylls and carotenoids in crude extracts by fitting with Gauss peak spectra. *Anal. Chem.* **2007**, *79*, 7611–7627. [CrossRef]
37. Genty, B.; Briantais, J.-M.; Baker, N.R. The relationship between the quantum yield of photosynthetic electron transport and quenching of chlorophyll fluorescence. *BBA-Gen. Subjects* **1989**, *990*, 87–92. [CrossRef]
38. Eilers, P.; Peeters, J. A model for the relationship between light intensity and the rate of photosynthesis in phytoplankton. *Ecol. Model.* **1988**, *42*, 199–215. [CrossRef]
39. Rodriguez, F.; Chauton, M.; Johnsen, G.; Andresen, K.; Olsen, L.; Zapata, M. Photoacclimation in phytoplankton: Implications for biomass estimates, pigment functionality and chemotaxonomy. *Mar. Biol.* **2006**, *148*, 963–971. [CrossRef]
40. Marie-Rose Vandenhecke, J.; Bastedo, J.; Cockshutt, A.M.; Campbell, D.A.; Huot, Y. Changes in the Rubisco to photosystem ratio dominates photoacclimation across phytoplankton taxa. *Photosynth. Res.* **2015**, *124*, 275–291. [CrossRef]
41. Andresen, E.; Lohscheider, J.; Šetlikova, E.; Adamska, I.; Šimek, M.; Küpper, H. Acclimation of *Trichodesmium erythraeum* ISM101 to high and low irradiance analysed on the physiological, biophysical and biochemical level. *New Phytol.* **2010**, *185*, 173–188. [CrossRef]

42. Walker, B.J.; Strand, D.D.; Kramer, D.M.; Cousins, A.B. The response of cyclic electron flow around photosystem I to changes in photorespiration and nitrate assimilation. *Plant Physiol.* **2014**, *165*, 453–462. [CrossRef]
43. Fujita, Y. A study on the dynamic features of photosystem stoichiometry: Accomplishments and problems for future studies. *Photosynth. Res.* **1997**, *53*, 83–93. [CrossRef]
44. Xu, J.; Gao, K. Future CO_2-induced ocean acidification mediates the physiological performance of a green tide alga. *Plant Physiol.* **2012**, *160*, 1762–1769. [CrossRef] [PubMed]
45. Price, G.D.; Badger, M.R.; Woodger, F.J.; Long, B.M. Advances in understanding the cyanobacterial CO_2-concentrating-mechanism (CCM): Functional components, Ci transporters, diversity, genetic regulation and prospects for engineering into plants. *J. Exp. Bot.* **2008**, *59*, 1441–1461. [CrossRef] [PubMed]
46. Hopkinson, B.M.; Dupont, C.L.; Allen, A.E.; Morel, F.M.M. Efficiency of the CO_2-concentrating mechanism of diatoms. *Proc. Natl. Acad. Sci. USA* **2011**, *108*, 3830–3837. [CrossRef] [PubMed]
47. Wu, Y.; Gao, K.; Riebesell, U. CO_2-induced seawater acidification affects physiological performance of the marine diatom *Phaeodactylum tricornutum*. *Biogeosciences* **2010**, *7*, 2915–2923. [CrossRef]
48. Suffrian, K.; Schulz, K.G.; Gutowska, M.; Riebesell, U.; Bleich, M. Cellular pH measurements in *Emiliania huxleyi* reveal pronounced membrane proton permeability. *New Phytol.* **2011**, *190*, 595–608. [CrossRef]
49. Flynn, K.J.; Blackford, J.C.; Baird, M.E.; Raven, J.A.; Clark, D.R.; Beardall, J.; Brownlee, C.; Fabian, H.; Wheeler, G.L. Changes in pH at the exterior surface of plankton with ocean acidification. *Nat. Clim. Chang.* **2012**, *2*, 510–513. [CrossRef]
50. Raven, J.A.; Giordano, M.; Beardall, J.; Maberly, S.C. Algal evolution in relation to atmospheric CO2: Carboxylases, carbon-concentrating mechanisms and carbon oxidation cycles. *Philos. Trans. R. Soc. B* **2012**, *367*, 493–507. [CrossRef]
51. Liu, N.; Beardall, J.; Gao, K. Elevated CO_2 and associated seawater chemistry do not benefit a model diatom grown with increased availability of light. *Aquat. Microb. Ecol.* **2017**, *79*, 137–147. [CrossRef]
52. Sun, J.-Z.; Wang, T.; Huang, R.; Yi, X.; Zhang, D.; Beardall, J.; Hutchins, D.A.; Liu, X.; Wang, X.; Deng, Z.; et al. Enhancement of diatom growth and phytoplankton productivity with reduced O_2 availability is moderated by rising CO_2. *Commun. Biol.* **2022**, *5*, 54. [CrossRef]

Disclaimer/Publisher's Note: The statements, opinions and data contained in all publications are solely those of the individual author(s) and contributor(s) and not of MDPI and/or the editor(s). MDPI and/or the editor(s) disclaim responsibility for any injury to people or property resulting from any ideas, methods, instructions or products referred to in the content.